Information Sciences 755 (2026) 123802

Contents lists available at ScienceDirect

Information Sciences

journal homepage: www.elsevier.com/locate/ins

Data-driven point-to-point iterative learning control for nonlinear systems subject to physical-layer FDI attacks and fading channels ☆

Lijuan Zha [a], Shuyi Huang [a], Jinliang Liu [b,*], Chen Peng [c]

[a] College of Science, Nanjing Forestry University, Nanjing, 210037, China
[b] School of Computer Science, Nanjing University of Information Science and Technology, Nanjing, 210044, China
[c] School of Mechatronic Engineering and Automation, Department of Automation, Shanghai University, Shanghai, 200444, China

HIGHLIGHTS

- Propose a statistical ramp-type FDI attack model using historical data.
- Introduce an unbiased correction for multiplicative channel fading.
- Develop a secure data-driven PTPFILC for finite-iteration PTP tracking.

ARTICLE INFO

Keywords:
Data-driven
Finite-iteration control
Additive attack
Multiplicative fading

ABSTRACT

This paper proposes a novel data-driven point-to-point finite-iteration learning control scheme for unknown nonlinear discrete-time repetitive systems operating under the coupled interference of physical-layer false data injection attacks and channel fading. A unified system framework is first established by integrating a ramp-type false data injection attack model and a channel fading model. To mitigate signal distortion induced by channel fading, an unbiased correction mechanism is introduced to reconstruct reliable data reflecting the physical-layer output corrupted by false data injection attacks. A dual-update strategy is further developed to simultaneously update the control input and parameter estimation. Convergence analysis demonstrates that once the number of iterations exceeds a predefined threshold, the corrected tracking error at specified tracking points will satisfy the prescribed accuracy requirements, thereby achieving the point-to-point finite-iteration tracking objective. Finally, simulation studies validate the effectiveness of the proposed method. The results show that the proposed scheme drives the tracking mean square error below 0.01 within 20 iterations for nonlinear discrete-time systems, outperforming existing methods in convergence speed. For the single-link robotic system, it realizes stable angular velocity tracking within 100 iterations and exhibits strong robustness over the attack coefficient range of 3 to 12.

1. Introduction

Accurate tracking control of nonlinear systems [1] is a fundamental technical requirement in complex engineering applications. Among various control strategies, iterative learning control (ILC) [2] has emerged as an effective solution for repetitive nonlinear

☆ This work was supported in part by the National Natural Science Foundation of China under Grants 62273174 and 62373252; in part by the Natural Science Foundation of Jiangsu Province of China under Grant BK20230063.
* Corresponding author.
Email address: liujinliang@vip.163.com (J. Liu).

https://doi.org/10.1016/j.ins.2026.123802
Received 22 March 2026; Received in revised form 7 June 2026; Accepted 16 June 2026
Available online 17 June 2026

systems, as it progressively improves tracking performance by exploiting data accumulated over successive iterations. Over the past decades, ILC has achieved significant advancements in both theoretical research [3] and practical applications [4]. For example, the work in [5] presents an adaptive quantization encoding–decoding mechanism that addresses several limitations of conventional quantized ILC, including excessive dependence on offline parameters, susceptibility to saturation, and stringent constraints on initial inputs.

While conventional ILC achieves excellent full-domain tracking performance, it inevitably incurs redundant computational overhead and unnecessary resource consumption in applications where stringent precision is required exclusively at specific time instants. Typical examples include the precise alignment phase in robotic arm assembly or the critical mission nodes in unmanned aerial vehicle operations. This practical need motivates point-to-point (PTP) tracking control, a more resource-efficient paradigm that optimizes performance only at designated time instants. Compared with full-time domain tracking [6], PTP tracking control [7] reduces computational demands, conserves control resources, and improves efficiency by focusing accuracy requirements on critical nodes while relaxing tolerances during non-critical periods. Despite these benefits, most existing ILC schemes are designed for full-domain tracking, making them ill-suited to the specific demands of PTP scenarios. This gap motivates the investigation of dedicated PTP-oriented ILC strategies.

In practical engineering scenarios, PTP tracking is usually implemented via wireless communication networks. However, such networks are inevitably subject to network-induced uncertainties, thereby resulting in the distortion of system output signals. Among these uncertainties, channel fading [8] over communication links is a pervasive issue that can severely attenuate transmitted signals, consequently degrading overall control performance. To address this issue, various approaches have been developed in existing results. For example, [9] employs a probability distribution model and develops a minimum-variance optimal linear estimator for random time-delay systems subject to measurement fading. In [10], channel fading is modeled as bounded uncertainty, and a distributed ensemble filter is designed for wireless sensor networks experiencing both channel fading and denial-of-service (DoS) attacks. The minimal average transmit power for mean-square stabilization is investigated in [11] for discrete-time linear systems over time-varying block-fading channels with additive white Gaussian noise. Despite these advances, ILC techniques that explicitly incorporate channel fading effects remain scarce, representing a promising yet underexplored research direction.

Apart from channel fading, network transmission links are also vulnerable to diverse malicious cyber threats [12], such as DoS attacks [13], data tampering and privacy leakage [14]. Among various malicious behaviors, false data injection (FDI) attacks [15] are characterized by high concealment and severe destructive effects. Such attacks implant false data by tampering with measurement data or control signals, which further lead to abnormal and unstable system operation. Existing literature has thoroughly explored the adverse effects of separate channel fading [16] or individual FDI attacks [17] on networked systems. However, the majority of current studies merely concentrate on the effect of FDI on systems, while neglecting the coupled interaction between channel fading and stealthy FDI deception attacks. Consequently, comprehensive investigations and systematic theoretical analyses on the simultaneous existence of wireless channel degradation and malicious FDI attacks are still inadequate, leaving significant room for further research and optimization.

Furthermore, it is worth noting that explicit and accurate system modeling remains challenging in practical scenarios with complex coupled disturbances [18], such as intelligent manufacturing [19] and industrial production systems [20]. To address this inherent difficulty, researchers have recently turned their attention to data-driven control methodologies [21], which leverage online input–output data to obviate the need for precise system dynamics. Specifically, [22] proposed a novel point-to-point finite-iteration learning control (PTPFILC) algorithm with output saturation for unknown nonlinear discrete-time systems. [23] presented a data-driven high-order PTPFILC scheme for unknown multi-input multi-output non-affine nonlinear repetitive discrete-time systems. Despite these notable advances in data-driven ILC design, few studies have considered the synergistic effects of channel fading and physical-layer FDI attacks within the data-driven ILC framework for unknown nonlinear discrete-time repetitive systems, thereby leaving a critical research gap.

To concurrently address the aforementioned challenges, this paper proposes a PTPFILC scheme for unknown nonlinear discrete-time repetitive systems subject to the coexistence of physical-layer FDI attacks and multiplicative channel fading. The primary contributions distinguishing this work from existing research are threefold.

1) Different from the conventional FDI attack models adopted in most existing studies, such as [24,25], this paper employs a ramp-type FDI attack model. This model is formulated based on the statistical characteristics (standard deviation) of historical data from the system physical-layer output and the duration interval of the attack, which characterizes the slowly varying and stealthy physical-layer data tampering behavior and is more consistent with practical cyber-attack scenarios.
2) While channel fading has been investigated in prior studies [26], the design of an unbiased correction mechanism for multiplicative fading remains largely unaddressed in the literature. In contrast to [26], this paper develops an unbiased correction strategy to achieve mean compensation for faded signals and alleviate signal distortion caused by multiplicative channel fading.
3) By simultaneously considering physical-layer FDI attacks and multiplicative channel fading, this work proposes a novel data-driven PTPFILC approach. The proposed method achieves high-precision PTP tracking at specified time instants within a finite number of iterations, while effectively mitigating system disturbances caused by both FDI attacks and channel fading.

To clarify the academic positioning of this work, the proposed framework is situated at the intersection of four advanced research domains. Specifically, it adopts PTPILC [27] as its overarching control paradigm and employs a model-free data-driven methodology to bypass the reliance on precise system dynamics. Furthermore, the scheme is categorized as a finite-iteration convergent control strategy in terms of its performance objective at designated critical nodes, while intrinsically serving as a robust anti-interference mechanism to ensure security resilience against the coupled cyber-physical threats of stealthy FDI attacks and multiplicative channel fading.

2. Problem formulation

Consider the following unknown nonlinear discrete-time repetitive system:

$$y_i(t+1) = f\left(y_i(t), u_i(t)\right), \tag{1}$$

where $i \in \mathbb{Z}_+$ denotes the iteration index, $t \in \{0, 1, \dots, T\}$ is the sampling time index, $y_i(t) \in \mathbb{R}$ is the physical-layer output, $u_i(t) \in \mathbb{R}$ is the system control input, and $f(\cdot)$ is an unknown nonlinear continuous function. The system dynamics are not assumed to be known to the controller and only input–output data collected over iterations are used for controller design.

During data acquisition or transmission, the physical output may be corrupted by a stealthy additive FDI attack. In this paper, the attack signal is modeled as a statistics-dependent additive perturbation whose magnitude is related to the standard deviation of recent output data. Therefore, the ramp-type FDI attack model [28] is adopted to describe the attack behavior as follows:

$$a_i(t) = \begin{cases} 0, & t \notin \mathcal{T}_{ai} \\ \alpha\sigma\left(y_i(t-t_{ap} : t)\right), & t \in \mathcal{T}_{ai} \end{cases} \tag{2}$$

where $t_{ap} < T$ is the attack preparation duration, $\mathcal{T}_{ai}$ is the attack injection time interval $[t_a, t_b]$ $(0 < t_a < t_b < T)$, α is the physical-layer attack intensity coefficient, $\sigma(\cdot)$ is the standard deviation of physical-layer output data and $y_i(t-t_{ap} : t)$ represents the real output data of the physical layer during $[t-t_{ap}, t]$.

Remark 1. The attack model in (2) is derived from the typical stealthy smart FDI attack model proposed in [28], which gradually tampers with system output data by altering the statistical characteristics of measurement data over time. Distinct from conventional abrupt FDI attacks, this ramp-type attack exhibits slow and continuous variation, rendering it more consistent with practical stealthy cyber-attack scenarios that can easily bypass traditional detection schemes. Therefore, we employ it to characterize the highly concealed physical-layer data tampering behavior and enhance the practicality of security control research. For the detailed design of the ramp-type FDI attack, readers can refer to the smart FDI attack modeling method for measurement data in smart grids [28].

Under the FDI attacks in (2), the output data is expressed as

$$y_i^*(t) = y_i(t) + a_i(t), \tag{3}$$

where $y_i^*(t)$ denotes the physical-layer output of the system corrupted by FDI attacks, and $a_i(t)$ represents the malicious attack signal injected at the time instant t.

Assumption 1 ([29]). There exists a constant $A_{\max} > 0$ such that $|a_i(t)| \le A_{\max}$ for all i and t, which reflects the boundedness of the actual attack intensity in practical systems.

Considering that signal transmission in practical engineering is often affected by channel fading, and to better align with real application scenarios, this study incorporates channel fading into the system model. The attacked signal transmitted over fading channels can be modeled as

$$y_i^f(t) = \beta_i(t) y_i^*(t), \tag{4}$$

where $y_i^f(t)$ represents the output data affected by physical-layer FDI attacks and channel fading. $\beta_i(t)$ is an independent and identically distributed random variable, which is independent of both the iteration index i and the time index t. The statistical characteristics satisfy $\mathbb{E}[\beta_i(t)] = \mu_\beta$, $\mathbb{E}[(\beta_i(t) - \mu_\beta)^2] = \sigma_\beta^2$, and $\mathbb{P}(\beta_i(t) > 0) = 1$, where μ_β is a known quantity [30]. The known mean value μ_β of the fading coefficient can be obtained through offline channel measurements or online statistical estimation, which provides a prerequisite for the design of the subsequent unbiased correction mechanism.

Remark 2. In case the communication channel is also affected by the FDI attacks, the overall received signal becomes $y_i^f(t) = \beta_i(t)\left(y_i(t) + a_i(t)\right) + a_i^c(t)$, where $a_i^c(t)$ denotes the communication-layer attack signal. Our data-driven approach, which compensates for both unknown nonlinearities and adversarial perturbations, can also estimate and mitigate this composite attack. To simplify the analysis, this work only discusses the effect of FDI attacks $a_i(t)$ in (2).

Remark 3. It is assumed that the channel fading coefficient $\beta_i(t)$ satisfies the upper bound $\beta_i(t) \le B_{max}$, where $B_{max} > 0$ is a constant. This bound stems from the physical limitations of channel fading coefficients in practical communication systems, such as channel gain, path loss, and antenna characteristics, and the existence of this bound precludes non-physical signal distortion caused by extreme channel fading. In the subsequent convergence analysis, this upper bound is employed to control the interference term introduced by random channel fading, thereby ensuring the uniform boundedness of both estimation and tracking errors. In practical implementations, B_{max} may be determined based on the worst-case channel fading margin of the channel or the statistical extremes of historical observational data.

To eliminate the signal bias caused by channel fading, an unbiased correction mechanism is applied to the faded signal received by the controller, and the corrected signal is given as [30]:

$$y_i^c(t) = \mu_\beta^{-1} y_i^f(t), \tag{5}$$

where $y_i^c(t)$ is the corrected signal. From the expected characteristic $\mathbb{E}[y_i^c(t)] = \mathbb{E}[\mu_\beta^{-1}\beta_i(t)y_i^*(t)] = y_i^*(t)$, it should be emphasized that this mechanism does not remove the FDI attacks. Instead, it provides a fading-compensated representation of the FDI-corrupted output for the subsequent learning update.

Remark 4. Although the proposed unbiased correction mechanism can theoretically mitigate the signal distortion caused by multiplicative channel fading, it has certain practical limitations. In real communication scenarios, channel noise always exists. If the signal attenuation induced by severe fading is so significant that a received signal power drops to the level comparable to channel noise, the useful signal and noise will become indistinguishable. In this case, reliable signal recovery cannot be realized even with the unbiased correction. Therefore, the effectiveness of the proposed method is based on the premise that the faded signal is still distinguishable from channel noise, which reflects a practical constraint of the data-driven correction strategy.

The relationship between the input and output sequences at the specified time instants in each iteration can be easily derived as:

$$\begin{aligned} y_i^c(t_s) &= \mu_\beta^{-1}\beta_i(t_s)y_i^*(t_s) \\ &= w_{t_s-1}^c(y_i(0), u_i(0), u_i(1), \dots, u_i(t_s-1), a_i(1), a_i(2), \dots, a_i(t_s), \beta_i(1), \beta_i(2), \dots, \beta_i(t_s)), \end{aligned} \tag{6}$$

where $t_s \in T^s = \{t_1, t_2, \dots, t_n\}(t_n \le T)$, $s = 1, 2, \dots, n$, and T^s is a given set of specified moments.

Let $Y_i^c = [y_i^c(t_1), y_i^c(t_2), \dots, y_i^c(t_n)]^{\mathrm{T}}$, then (6) can be rewritten in a vector form as:

$$Y_i^c = W^c(y_i(0), U_i^{\mathrm{T}}, A_i^{\mathrm{T}}, B_i^{\mathrm{T}}), \tag{7}$$

where $U_i = [u_i(0), u_i(1), \dots, u_i(N-1)]^{\mathrm{T}} \in \mathbb{R}^N$, $A_i = [a_i(1), a_i(2), \dots, a_i(N)]^{\mathrm{T}} \in \mathbb{R}^N$, $B_i = [\beta_i(1), \beta_i(2), \dots, \beta_i(N)]^{\mathrm{T}}$, and $W^c(\cdot) = [w_{t_1-1}^c(\cdot), w_{t_2-1}^c(\cdot), \dots, w_{t_n-1}^c(\cdot)]^{\mathrm{T}}$ denotes the unknown vector function.

Assumption 2 ([22]). The initial physical-layer output of the system in each iteration satisfies $y_i(0) = y_0$, ensuring the repeatability of the iteration process.

Assumption 3 ([22]). The unknown vector function $W^c(\cdot)$ satisfies the generalized Lipschitz condition with respect to the control input sequence U_i, the FDI attack sequence A_i, and the channel fading sequence B_i, that is

$$\|W^c(y_1, U_1, A_1, B_1) - W^c(y_2, U_2, A_2, B_2)\| \le L_y|y_1 - y_2| + L_U\|U_1 - U_2\| + L_A\|A_1 - A_2\| + L_B\|B_1 - B_2\|$$

where $L_y, L_U, L_A, L_B > 0$ are positive Lipschitz constants.

Assumption 4 ([22]). The partial derivatives of the function $W^c(\cdot)$ with respect to each of the components are bounded, non-zero, and their signs remain constant.

Remark 5. Assumption 2 guarantees consistent initial conditions for the iterative process, satisfying the repeatability requirement of ILC. In many repetitive operation scenarios, such as robot grasping, press cycles, and trajectory scanning, the system can return to a fixed initial state through reset, zeroing, and other operations before each task begins. Therefore, this assumption can be implemented in engineering. Assumption 3 introduces a generalized Lipschitz condition, which is reasonable and standard in engineering practice and nonlinear control theory. Assumption 3 is widely adopted in model-free adaptive control for nonlinear systems, reflects the bounded rate of change of system output with respect to control input, FDI attacks, and channel fading, and provides essential mathematical guarantees for the boundedness analysis and convergence proof of the proposed data-driven PTP ILC scheme. Assumption 4 constrains the partial derivatives of the system's unknown dynamics, ensuring the implementability and convergence of the iterative learning law. All three assumptions, which have also been used in [22,23], are standard engineering assumptions in the control community and consistent with the characteristics of practical systems.

Based on Assumption 2 and the differential mean value theorem, from (7), one can derive

$$\begin{aligned} \Delta Y_i^c &= \frac{\partial W^c}{\partial U_i^{\mathrm{T}}}\Delta U_i + \frac{\partial W^c}{\partial A_i^{\mathrm{T}}}\Delta A_i + \frac{\partial W^c}{\partial B_i^{\mathrm{T}}}\Delta B_i \\ &= \Phi_i \Delta Z_i, \end{aligned} \tag{8}$$

where $\Delta Y_i^c = Y_i^c - Y_{i-1}^c$, $\Delta Z_i = [\Delta U_i, \Delta A_i, \Delta B_i]^{\mathrm{T}}$. The time-varying parameter matrix Φ_i satisfies $\Phi_i = [\partial W^c/\partial U_i^{\mathrm{T}}, \partial W^c/\partial A_i^{\mathrm{T}}, \partial W^c/\partial B_i^{\mathrm{T}}] = [\Phi_i^U, \Phi_i^A, \Phi_i^B]$. The dimensions of the submatrices Φ_i^U, Φ_i^A and Φ_i^B are $n \times T$. If the number of columns in row s is less than T, pad the row with zeros to compensate for the dimension mismatch.

For convenience, let $\phi_i(s) = [\partial w_{t_s-1}^c/\partial u_i(0), \dots, \partial w_{t_s-1}^c/\partial u_i(t_s-1), \partial w_{t_s-1}^c/\partial a_i(1), \dots, \partial w_{t_s-1}^c/\partial a_i(t_s), \partial w_{t_s-1}^c/\partial \beta_i(1), \dots, \partial w_{t_s-1}^c/\partial \beta_i(t_s)] = [\phi_i^U(s), \phi_i^A(s), \phi_i^B(s)]$, $\Delta Z_i(t_s-1) = [\Delta u_i(0), \dots, \Delta u_i(t_s-1), \Delta a_i(1), \dots, \Delta a_i(t_s), \Delta\beta_i(1), \dots, \Delta\beta_i(t_s)]^{\mathrm{T}} = [\Delta U_i^{\mathrm{T}}(t_s-1), \Delta A_i^{\mathrm{T}}(t_s-1), \Delta B_i^{\mathrm{T}}(t_s-1)]^{\mathrm{T}}$, (8) can be rewritten as a scalar form

$$\Delta y_i^c(t_s) = \phi_i(s)\Delta Z_i(t_s-1), \tag{9}$$

where $\Delta y_i^c(t_s)$ represents the corrected output increment at the specified tracking time t_s of the i-th iteration, which directly characterizes the output variation at the critical node, and $\Delta Z_i(t_s-1)$ denotes the composite increment vector that integrates the incremental information of the control input, FDI attack and channel fading, with a linear mapping relationship established between them through $\phi_i(s)$.

Our objective is to design a data-driven PTPFILC scheme for unknown nonlinear discrete-time repetitive systems subject to both physical-layer FDI attacks and multiplicative channel fading. The control objective is to ensure that the system output $y_i^c(t_s)$ tracks the desired value $y_d(t_s)$ at the specified time instants, and that the tracking error $e_i(t_s) = y_d(t_s) - y_i^c(t_s)$ converges to a stable region within a finite number of iterations.

3. Controller design

This section develops a data-driven learning law for PTP tracking. Since the system dynamics and the parameters are unknown, the proposed controller updates the control input and parameter estimation simultaneously using the corrected input–output data. The effects of FDI attacks and fading-channel fluctuations are treated as bounded disturbances in the learning process.

3.1. Control input update

For the s-th PTP interval $[t_{s-1}, t_s - 1]$, with $t_0 = 0$, the control input segment is defined as $U_i(t_s - t_{s-1}) = [u_i(t_{s-1}), u_i(t_{s-1}+1), \dots, u_i(t_s - 1)]^{\mathrm{T}}$. The following cost function is constructed to update the control input:

$$\begin{aligned} &J(U_i(t_s - t_{s-1})) \\ &= \left|y_d(t_s) - y_i^c(t_s)\right|^2 + \lambda \left\|\Delta U_i(t_s - t_{s-1})\right\|^2 \\ &= \left|e_{i-1}(t_s) - \phi_i(s)\Delta Z_i(t_s - 1)\right|^2 + \lambda \left\|\Delta U_i(t_s - t_{s-1})\right\|^2, \end{aligned} \tag{10}$$

where $\lambda > 0$ is a weighting factor used to limit changes in $U_i(t_s - t_{s-1})$.

Set the partial derivative of the cost function (10) with respect to $U_i(t_s - t_{s-1})$ to be zero. Consequently, the following control algorithm can be obtained

$$U_i(t_s - t_{s-1}) = U_{i-1}(t_s - t_{s-1}) + \frac{\rho \phi_i^{U,\mathrm{T}}(s) e_{i-1}(t_s)}{\lambda + \left\|\phi_i^U(s)\right\|^2}, \tag{11}$$

where $\rho \in (0,1)$ is the size of the learning step.

3.2. Parameter estimation update

In order to implement (11), the value of $\phi_i^U(s)$ is required to be known in advance. Therefore, we design the following performance index function to estimate its value

$$J(\hat{\phi}_i^U(s)) = \left\|\Delta y_{i-1}^c(t_s) - \hat{\phi}_i^U(s)\Delta U_{i-1}(t_s - 1)\right\|^2 + \mu \left\|\hat{\phi}_i^U(s) - \hat{\phi}_{i-1}^U(s)\right\|^2. \tag{12}$$

Following the same derivation steps as in (10) and (11), we can derive

$$\hat{\phi}_i^U(s) = \hat{\phi}_{i-1}^U(s) + \frac{\eta \Delta y_{i-1}^c(t_s)\Delta U_{i-1}^{\mathrm{T}}(t_s - 1)}{\mu + \left\|\Delta U_{i-1}(t_s - 1)\right\|^2} - \frac{\eta \hat{\phi}_{i-1}^U(s)\Delta U_{i-1}(t_s - 1)\ \Delta U_{i-1}^{\mathrm{T}}(t_s - 1)}{\mu + \left\|\Delta U_{i-1}(t_s - 1)\right\|^2}, \tag{13}$$

where $\hat{\phi}_i^U$ is the parameter estimate at the i-th iteration, $\eta \in (0,1)$ is the estimation step size, $\mu > 0$ is the regularization coefficient.

Combining the control input update law in (11) and the parameter estimate update law with the reset mechanism in (13), the complete data-driven PTPFILC scheme for nonlinear systems under physical-layer FDI attacks and channel fading is formulated as:

$$\hat{\phi}_i^U(s) = \hat{\phi}_{i-1}^U(s) + \frac{\eta \Delta y_{i-1}^c(t_s)\Delta U_{i-1}^{\mathrm{T}}(t_s - 1)}{\mu + \left\|\Delta U_{i-1}(t_s - 1)\right\|^2} - \frac{\eta \hat{\phi}_{i-1}^U(s)\Delta U_{i-1}(t_s - 1)\ \Delta U_{i-1}^{\mathrm{T}}(t_s - 1)}{\mu + \left\|\Delta U_{i-1}(t_s - 1)\right\|^2}, \tag{14}$$

$$\hat{\phi}_i^U(s) = \hat{\phi}_0^U(s),\ \text{if } sign(\hat{\varphi}_i(\tau)) \neq sign(\hat{\varphi}_0(\tau)) \text{ or } \left\|\hat{\phi}_i^U(s)\right\| \le \zeta \text{ or } \left\|\Delta U_{i-1}(t_s - 1)\right\| \le \zeta,$$

$$U_i(t_s - t_{s-1}) = U_{i-1}(t_s - t_{s-1}) + \frac{\rho \hat{\phi}_i^{U,\mathrm{T}}(s) e_{i-1}(t_s)}{\lambda + \left\|\hat{\phi}_i^U(s)\right\|^2}, \tag{15}$$

where $\varphi_i(\tau) = \partial w_{t_s-1}^c / \partial u_i(\tau)$, $\hat{\phi}_0^U(s)$ is the initial value of $\hat{\phi}_i^U(s)$, and $\zeta > 0$ is a sufficiently small constant.

Remark 6. The condition $sign(\hat{\varphi}_i(\tau)) \neq sign(\hat{\varphi}_0(\tau))$ identifies a directional deviation in the parameter estimation. According to Assumption 4, the partial derivatives of the function $w^c(\cdot)$ with respect to input components are bounded, non-zero, and possess constant signs. The initial estimation $\hat{\varphi}_0(\tau)$ is configured to match the true sign of $\varphi_i(\tau)$, based on prior knowledge or preliminary system analysis. A sign reversal of $\hat{\varphi}_i(\tau)$ during iteration signals a significant estimation error, such as misjudging the positive/negative correlation between control input and system output. Without resetting, this directional error can lead to improper control input adjustments, causing divergent tracking errors. Restoring the initial sign $\hat{\varphi}_0(\tau)$ reestablishes correct directional guidance for the learning law, thereby preventing cumulative errors arising from misestimation.

Algorithm 1 Data-driven PTPFILC.

Input: Desired tracking instants $T^s = \{t_1, t_2, \dots, t_n\}$, parameters $\rho, \lambda, \eta, \mu, \zeta$, initialization $y_i(0), u_0(t), \hat{\varphi}_0(\tau)$, and maximum number of iteration i_{max}.
Output: Optimal control input sequence U_{i+1} fulfilling PTP tracking accuracy.
Initialization: Set iteration index $i = 0$.
While $i \le i_{max}$ **do**
  Apply control input $u_i(t)$ to the physical system.
  System physical-layer output $y_i(t)$ is compromised by a ramp-type FDI attack, yielding $y_i^*(t)$.
  Transmit $y_i^*(t)$ over the fading channel to obtain the received signal $y_i^f(t)$.
  Reconstruct the corrected output via $y_i^c(t) = \mu_\beta^{-1} y_i^f(t)$.
  If $i > 0$, compute $\hat{\phi}_i^U(s)$ dynamically using the update law and reset mechanism formulated in (14).
  Calculate the PTP tracking error $e_i(t_s) = y_d(t_s) - y_i^c(t_s)$.
  Synthesize the control input for the next iteration $U_{i+1}(t_s - t_{s-1})$ utilizing the dual-update strategy in (15).
  Update iteration index $i \leftarrow i + 1$.
end While

Remark 7. The parameter reset mechanism triggered by sign inconsistency is applicable only to temporary sign reversals induced by short-term, weak attacks. In such scenarios, the attack does not alter the intrinsic characteristics of the system but merely causes sign misjudgment through FDI attacks. Moreover, the attack duration is shorter than the iterative convergence cycle. Under these conditions, resetting to the initial sign consistent with the true system characteristics can promptly restore the correct control direction. When combined with the dual-update mechanism, this enables the system to quickly reenter its optimization trajectory.

Algorithm 1 outlines the simulation process of the proposed PTPFILC. This structured procedural framework encapsulates the complete implementation logic of the method, serving to simulate and evaluate the performance of PTPFILC under the influence of FDI attacks and channel fading.

4. Convergence analysis

In this section, rigorous theoretical analysis is conducted to prove the boundedness of the parameter estimate and the finite-iteration convergence of the PTP tracking error for the proposed data-driven PTPFILC scheme. All analyses are carried out under Assumptions 1–4, which ensure the rationality and strictness of the theoretical results.

Theorem 1. *Under Assumption 1–4, the parameter estimate $\hat{\phi}_i^U(s)$ obtained by the update law in (14) is bounded in expectation for all i. That is, there exists a positive constant $B_\phi > 0$ such that $E\{||\hat{\phi}_i^U(s)||\} \le B_\phi$ holds for all i and all $t_s \in T^s$.*

Proof. Let $\tilde{\phi}_i^U(s) = \hat{\phi}_i^U(s) - \phi_i^U(s)$. Subtracting $\phi_i^U(s)$ from both sides of (14) and taking the mathematical expectation, we can obtain

$$\begin{aligned} E\left\{\tilde{\phi}_i^U(s)\right\} =& E\left\{\tilde{\phi}_{i-1}^U(s)\right\} - E\left\{\Delta\phi_i^U(s)\right\} + E\left\{\tilde{b}_{i-1}\right\} E\left\{\Delta y_{i-1}^c(t_s) - \hat{\phi}_{i-1}^U(s)\Delta \mathbf{U}_{i-1}(t_s-1)\right\} \\ =& E\left\{(I - b_{i-1})\tilde{\phi}_{i-1}^U(s)\right\} - E\left\{\Delta\phi_i^U(s)\right\} + E\left\{\tilde{b}_{i-1}\right\} \\ & \times E\left\{\phi_{i-1}^A(s)\Delta A_{i-1}(t_s-1) + \phi_{i-1}^B(s)\Delta B_{i-1}(t_s-1)\right\}, \end{aligned} \tag{16}$$

where $\Delta\phi_i^U(s) = \phi_i^U(s) - \phi_{i-1}^U(s)$, $b_{i-1} = \eta\Delta U_{i-1}(t_s-1)\Delta U_{i-1}^{\mathrm{T}}(t_s-1)/(\mu + \|\Delta U_{i-1}(t_s-1)\|^2)$ and $\tilde{b}_{i-1} = \eta\Delta U_{i-1}(t_s-1)/(\mu + \|\Delta U_{i-1}(t_s-1)\|^2)$. Since $\eta\|\Delta U_{i-1}(t_s-1)\|^2 < \|\Delta U_{i-1}(t_s-1)\|^2 < \mu + \|\Delta U_{i-1}(t_s-1)\|^2$, we have $0 < \|b_{i-1}\| < 1$. Moreover, $\eta\zeta^2/(\mu+\zeta^2)$ serves as a positive lower bound for $\|b_{i-1}\|$ according to the reset algorithm. Then, one has

$$0 \le \|I - b_{i-1}\| \le 1 - \frac{\eta\zeta^2}{\mu + \zeta^2} = c_1 < 1. \tag{17}$$

Recalling Assumption 3, we know that Φ_i is bounded, which implies that $||\phi_i^U||$, $||\phi_i^A||$ and $||\phi_i^B||$ are bounded. Therefore, we take l_u, l_A and l_B as the upper bounds of these, respectively. l_u, l_A and l_B are positive constants. For the interference term induced by FDI attacks and channel fading, applying the triangle inequality and Assumptions 1, we can derive its upper bound as:

$$\begin{aligned} & E\left\{\left\|\phi_{i-1}^A(s)\Delta A_{i-1}(t_s-1) + \phi_{i-1}^B(s)\Delta B_{i-1}(t_s-1)\right\|\right\} \\ \le & E\left\{\left\|\phi_{i-1}^A(s)\Delta A_{i-1}(t_s-1)\right\|\right\} + E\left\{\|\phi_{i-1}^B(s)\Delta B_{i-1}(t_s-1)\|\right\} \\ \le & 2\sqrt{T} l_A A_{max} + 2\sqrt{T} l_B B_{max} \triangleq D. \end{aligned} \tag{18}$$

Taking the norm of both sides of (16) and applying the triangle inequality of matrix norms, the expected value of the estimation error norm satisfies:

$$\begin{aligned}
&E\left\{\left\|\tilde{\phi}_i^U(s)\right\|\right\}\\
\le& c_1 E\left\{\left\|\tilde{\phi}_{i-1}^U(s)\right\|\right\}+E\left\{\left\|\Delta\phi_i^U(s)\right\|\right\}+\frac{\eta}{2\sqrt{\mu}}E\left\{\left\|\phi_{i-1}^A(s)\Delta A_{i-1}(t_s-1)+\phi_{i-1}^B(s)\Delta B_{i-1}(t_s-1)\right\|\right\}\\
\le& c_1 E\left\{\left\|\tilde{\phi}_{i-1}^U(s)\right\|\right\}+c_2,
\end{aligned}\tag{19}$$

where $c_2 = 2l_u + \eta D/(2\sqrt{\mu})$ is a positive constant.

By recursively expanding the inequality in (19), the expected value of the estimation error norm at the i-th iteration can be expressed as:

$$\begin{aligned}
E\left\{\left\|\tilde{\phi}_i^U(s)\right\|\right\} &\le c_1 E\left\{\left\|\tilde{\phi}_{i-1}^U(s)\right\|\right\}+c_2\\
&\le c_1^2 E\left\{\left\|\tilde{\phi}_{i-2}^U(s)\right\|\right\}+c_1c_2+c_2\\
&\le \cdots \le c_1^{i-1}E\left\{\left\|\tilde{\phi}_1^U(s)\right\|\right\}+\frac{c_2(1-c_1^{i-1})}{1-c_1}.
\end{aligned}\tag{20}$$

Since $c_1 < 1$, (20) reveals the boundedness of $\|\tilde{\phi}_i^U(s)\|$. Moreover, the boundedness of $\phi_i^U(s)$ also guarantees that $\hat{\phi}_i^U(s)$ is bounded. ∎

Based on the boundedness of the parameter estimation error established in Theorem 1, we proceed to analyze the finite-iteration convergence of the corrected PTP tracking error in the subsequent theorem. Specifically, by exploiting the boundedness of the parameter estimate and the proposed dual-update law, the tracking error at all specified time instants converges to a prescribed accuracy bound within a finite number of iterations, even in the presence of FDI attacks and channel fading. This analysis further corroborates the robustness and efficacy of the proposed data-driven PTP ILC framework.

Theorem 2. *Consider the nonlinear system (1) under the FDI attack and channel fading models in Eqs. (2)-(5). Suppose that Assumptions 1–4 hold and that the learning gain satisfies the required contraction condition. For the desired trajectory $y_d(t_s)$ at specified instants $t_s \in T^s$, if $\lambda > \lambda_{min}$ is selected, there exists a finite positive integer i^* such that the expected PTP tracking error converges to the prespecified accuracy, and the error satisfies $E\{|e_i(t_s)|\} \le \varepsilon$ for all $i > i^*$ and $t_s \in T^s$, where the upper bound of the error is determined by the coupled interference bound D of FDI attacks and multiplicative fading.*

Proof. Based on the system model in (9), the PTP tracking error at the i-th iteration can be rewritten as a recursive form related to the error at the $(i-1)$-th iteration

$$\begin{aligned}
e_i(t_s) =& e_{i-1}(t_s)-\phi_i(s)\Delta Z_i(t_s-1)\\
=& e_{i-1}(t_s)-\phi_i^U(s)\Delta U_i(t_s-1)-(\phi_i^A(s)\Delta A_{i-1}(t_s-1)+\phi_i^B(s)\Delta B_{i-1}(t_s-1))\\
=& e_{i-1}(t_s)-\frac{\rho\phi_i^U(s)\hat{\phi}_i^{U,\mathrm{T}}(s)e_{i-1}(t_s)}{\lambda+\|\hat{\phi}_i^U(s)\|^2}-(\phi_i^A(s)\Delta A_{i-1}(t_s-1)+\phi_i^B(s)\Delta B_{i-1}(t_s-1)).
\end{aligned}\tag{21}$$

Taking the mathematical expectation for both sides of (21), one has

$$E\left\{e_i(t_s)\right\}=\left(1-\frac{\rho\phi_i^U(s)\hat{\phi}_i^{U,\mathrm{T}}(s)}{\lambda+\left\|\hat{\phi}_i^U(s)\right\|^2}\right)E\left\{e_{i-1}(t_s)\right\}-E\left\{\phi_{i-1}^A(s)\Delta A_{i-1}(t_s-1)+\phi_{i-1}^B(s)\Delta B_{i-1}(t_s-1)\right\}.\tag{22}$$

From Assumption 4 and the parameter reset mechanism, one can deduce that $\phi_i^U(s)\hat{\phi}_i^{U,\mathrm{T}}(s) \ge 0$. Define a variable $\lambda_{min} = 0.25l_u^2$. If we choose a λ such that $\lambda > \lambda_{min}$, then there exists a constant $N \in (0,1)$ that satisfies

$$0 < N \le \frac{\phi_i^U(s)\hat{\phi}_i^{U,\mathrm{T}}(s)}{\lambda+\left\|\hat{\phi}_i^U(s)\right\|^2} \le \frac{l_u}{2\sqrt{\lambda}} < \frac{l_u}{2\sqrt{\lambda_{min}}} = 1.\tag{23}$$

Further, we have $\rho\phi_i^U(s)\hat{\phi}_i^{U,\mathrm{T}}(s)/(\lambda+||\hat{\phi}_i^U(s)||^2) < \rho l_u/(2\sqrt{\lambda_{min}}) \le 1$. Therefore, there exists a constant $c_3 \in (0,1)$ that satisfies

$$\left|1-\frac{\rho\phi_i^U(s)\hat{\phi}_i^{U,\mathrm{T}}(s)}{\lambda+\left\|\hat{\phi}_i^U(s)\right\|^2}\right| \le c_3 < 1.\tag{24}$$

Thus, it yields that

$$
\begin{aligned}
E\{|e_i(t_s)|\} &\le E\left\{|1 - \frac{\rho\phi_i^U(s)\hat{\phi}_i^{U,\mathrm{T}}(s)}{\lambda + \left\|\hat{\phi}_i^U(s)\right\|^2}|\right\} E\{|e_{i-1}(t_s)|\} + D \\
&\le c_3 E\{|e_{i-1}(t_s)|\} + D \\
&\le \cdots \le c_3^{i-1} E\{|e_1(t_s)|\} + \frac{D(1-c_3^{i-1})}{1-c_3}.
\end{aligned} \tag{25}
$$

The derived error recursion in (25), combined with Theorem 1, guarantees that the tracking error, control input, and parameter estimation error are all uniformly ultimately bounded in expectation, which serves as a rigorous metric of system stability in iterative learning. To achieve the PTP tracking objective, it should be satisfied that $E\{|e_i(t_s)|\} \le \varepsilon$, which only requires $c_3^{i-1}E\{|e_1(t_s)|\} + D(1 - c_3^{i-1})/(1-c_3) \le \varepsilon$. By calculation, we can obtain

$$
i \ge log_{c_3}\left(\frac{\varepsilon - \frac{D}{1-c_3}}{E\{|e_1(t_s)|\} - \frac{D}{1-c_3}}\right) + 1. \tag{26}
$$

Thus, i^* satisfies

$$
i^* = \left\lfloor \log_{c_3}\left(\frac{\varepsilon - \frac{D}{1-c_3}}{E\{|e_1(t_s)|\} - \frac{D}{1-c_3}}\right)\right\rfloor + 2, \tag{27}
$$

where $\lfloor\cdot\rfloor$ denotes the floor function. Since $\log_{c_3}(\cdot)$ is a finite value, i^* is a finite positive integer.

From the analytical expression of i^* in (27), it can be observed that the finite threshold i^* is co-determined by the prescribed accuracy ε, the initial tracking error, the robustness coefficient, and the upper bound of the coupled interference induced by FDI attacks and channel fading. The interaction between attack dynamics and learning convergence plays a dominant role in the entire iterative process. On one hand, the intensity and variation speed of FDI attacks reflect the real-time attack dynamics, which continuously affect the intensity of coupled interference and further influence the convergence speed of the ILC algorithm. On the other hand, the learning convergence behavior in turn suppresses the impact of attack dynamics by adjusting the control input and the parameter estimation, thereby forming a clear two-way interaction mechanism.

Specifically, a smaller prescribed accuracy ε or a stronger coupled interference will result in a larger i^*, implying that more iterations are required to achieve the desired tracking performance. As the attack dynamics intensify, the coupled interference becomes stronger, which slows down the learning convergence rate and increases the finite threshold i^*. Meanwhile, the proposed data-driven learning scheme can adaptively suppress the fluctuations caused by attack dynamics, which accelerates the convergence process and ensures that the learning convergence is not disrupted by real-time changes in attack dynamics. Furthermore, since i^* is a finite positive integer, it is theoretically guaranteed that the PTP tracking objective can be achieved within a finite number of iterations, which further validates the effectiveness of the proposed data-driven learning scheme.

To summarize, there exists a finite number of iterations i^* such that when $i > i^*$, the system achieves PTP finite-iteration tracking. ■

Remark 8. It should be noted that the proposed dual-update strategy is inherently robust against FDI attacks. Specifically, the adaptive parameter estimator, which is updated solely using input–output data, acts as an implicit disturbance observer to capture the combined effects of unknown plant dynamics and FDI attacks. Meanwhile, the iterative update law directly minimizes the tracking error caused by FDI attacks. As the iteration proceeds, the learning law adaptively generates feedforward compensation terms to counteract persistent attack signals, thereby suppressing their interference with tracking performance. Therefore, unlike the traditional attack detection–compensation framework, the proposed scheme does not require the explicit removal of FDI attacks from the output signals. Instead, it directly mitigates their adverse impact on tracking performance through the dual-update mechanism.

Theorem 3. *Under Assumptions 1–4 and the conditions of Theorem 2, the mean-square tracking error of the proposed data-driven PTPFILC scheme is uniformly ultimately bounded in expectation for all specified tracking instants* $t_s \in T^s$.

Proof. Define the Lyapunov candidate function along the iteration domain as $V_i = e_i^2(t_s)$. According to (21), the tracking error dynamics at the i-th iteration can be abstracted into the following recursive form

$$
e_i(t_s) = (1 - K_i)e_{i-1}(t_s) - d_{i-1}, \tag{28}
$$

where $K_i = (\rho\phi_i^U(s)\hat{\phi}_i^{U,\mathrm{T}}(s))/(\lambda + ||\hat{\phi}_i^U(s)||^2)$ and $d_{i-1} = \phi_i^A(s)\Delta A_{i-1}(t_s-1) + \phi_i^B(s)\Delta B_{i-1}(t_s-1)$. From (18), the disturbance term is bounded, and hence $E\{d_{i-1}^2\} \le \bar{D}$. Taking the square of both sides of (28) and applying Young's inequality, we obtain that

$$
e_i^2(t_s) = ((1-K_i)e_{i-1}(t_s) - d_{i-1})^2 \le (1+m)(1-K_i)^2 e_{i-1}^2(t_s) + (1+\frac{1}{m})d_{i-1}^2, \tag{29}
$$

where m is any positive constant. Substituting (29) into $V_i = e_i^2(t_s)$ and taking the mathematical expectation on both sides yields that

$$E\{V_i\} \leq (1+m)c_3^2 E\{V_{i-1}\} + (1+\frac{1}{m})\bar{D}. \tag{30}$$

Since $0 < c_3 < 1$, $c_3^2 < 1$. We can always find a sufficiently small positive constant m such that $0 < M \overset{\Delta}{=} (1+m)c_3^2 < 1$. Let $C \overset{\Delta}{=} (1+\frac{1}{m})\bar{D}$, (30) simplifies to

$$E\{V_i\} \leq M E\{V_{i-1}\} + C. \tag{31}$$

Taking the difference of V_i in the iteration domain and taking the expectation, one can get

$$E\{\Delta V_i\} \leq -(1-M)E\{V_{i-1}\} + C. \tag{32}$$

According to the above difference inequality (32), if the system error energy is sufficiently large such that $(1-M)E\{V_{i-1}\} > C$, then it strictly follows that $E\{\Delta V_i\} < 0$. This implies that as long as the error exceeds the bound determined by the disturbance C, the system energy will strictly decrease in the next iteration. As the iteration index $i \to \infty$, the error energy $E\{V_i\}$ will eventually converge to and remain within the set $\Omega = \{E\{V_i\} | E\{V_i\} \leq \frac{C}{1-M}\}$. This completes a rigorous proof that the mean-square tracking error of the system is uniformly ultimately bounded in expectation. Furthermore, from the perspective of input-to-state stability (ISS), this inequality dictates that the system dynamics along the iteration domain are ISS with respect to the coupled interference of FDI attacks and channel fading. That is, bounded cyber-physical disturbances merely lead to a bounded tracking error, fully demonstrating the exceptional robustness and stability resilience of the proposed control scheme. ■

5. Simulation results

To rigorously evaluate the efficacy of the proposed data-driven PTPFILC scheme, numerical simulation experiments are conducted in this section. The simulations examine the scheme's ability to suppress the coupled interference of physical-layer FDI attacks and communication fading, as well as its capacity to achieve high-precision PTP tracking within a limited number of iterations. The performance assessment primarily relies on the mean square error (MSE) of the tracking error and the system's convergence speed, which together provide a comprehensive verification of the proposed scheme's superiority in complex interference environments.

5.1. Numerical simulation

Consider a single-input single-output nonlinear discrete-time system

$$y_i(t+1) = \frac{y_i(t)}{1+y_i(t)^2} + u_i(t)^3, \tag{33}$$

where $t = \{1, 2, \ldots, 50\}$ denotes the running time and i denotes the number of iteration. The dynamic equation of the above system is unknown and is only used as a data generation tool in simulation testing. The desired trajectory is as follows

$$y_d(t+1) = 0.6\sin(\pi t/10) + 0.5\cos(\pi t/10). \tag{34}$$

We set the parameters in the control scheme (14)-(15) as $\rho = 0.5$, $\lambda = 0.8$, $\eta = 0.3$, $\mu = 0.8$, $\zeta = 10^{-6}$. The mathematical expectation for the decay coefficient is set to $\mu_\beta = 0.95$, with variance $\sigma_\beta = 0.1$. The attack coefficient, attack preparation time, and attack period are set to $\alpha = 4$, $t_{ap} = 5$ and $\mathcal{T}_{ai} = [15, 45]$, respectively.

In addition, the system initial output and input are $y_i(0) = 0$, $u_0(t) = 0.1$, respectively, which represent the value of the control output at the beginning of each iteration and the value of the control input at any time during the initial iteration. The initial estimate is $\hat{\varphi}_0(\tau) = 0.5$. For the PTP tracking task, we have designated five time intervals for simulation experiments, namely $t_1 = 10$, $t_2 = 20$, $t_3 = 30$, $t_4 = 40$ and $t_5 = 50$.

The iterative tracking performance is illustrated in Fig. 1, which depicts the MSE convergence trajectory. It can be observed that the error index exhibits a decreasing trend as the number of iterations increases, stabilizes near zero in the later stages, and verifies the convergence of the proposed algorithm. However, fluctuations still exist due to the influence of channel fading. To further illustrate the trajectory tracking performance of the proposed control strategy, the predictive PTP ILC (PPTPILC) [23] and high-order PTP ILC (HOPTPILC) [31] algorithms are selected as comparative methods for validation. For the PPTPILC algorithm, the prediction step sizes are configured as $N_y = 5$ and $N_u = 3$. For the HOPTPILC algorithm, the key parameters are the order $r = 3$, the weight vector $\alpha = [0.9, 0.09, 0.01]$, and $[\rho_4, \rho_5, \rho_6, \rho_7] = [0.3, 0.3, 0.4, 0.4]$. All other controller parameters are kept consistent with those of the proposed PTPFILC to ensure the fairness of the comparative simulation. The corresponding simulation results are presented in Fig. 1. It is evident that all three algorithms can achieve the convergence of tracking errors, and the proposed control strategy exhibits a faster convergence speed. The worse performance of the two comparative algorithms stems from their lack of unbiased correction mechanisms for channel fading mean and dedicated suppression against FDI attacks, which in turn verifies the effectiveness of the unbiased correction and dual-update strategy introduced in this work. Fig. 2 illustrates that, despite the coupled interference of FDI attacks and channel fading substantially increasing the system's control complexity, the algorithm developed herein still enables error convergence within a finite number of iterations. This result highlights the algorithm's robustness advantage when operating in complex interference environments.

To verify the robustness of the proposed scheme against communication fading, we conducted the following simulation experiments. It should be clarified that the severity of communication fading is characterized by both the expected value of the channel

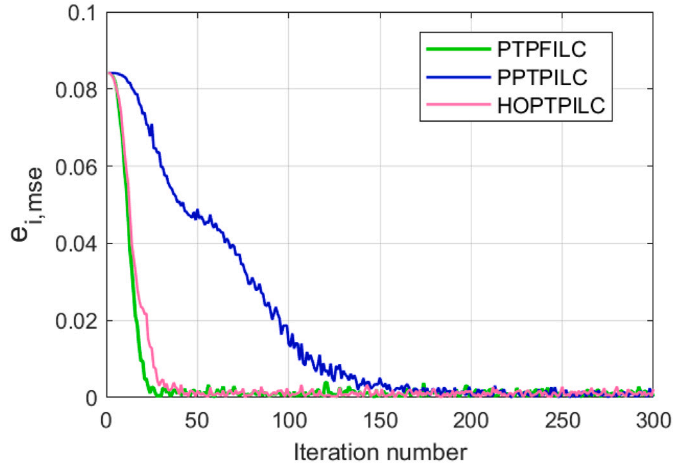

Fig. 1. MSE convergence curves of the system under FDI attacks and channel fading.

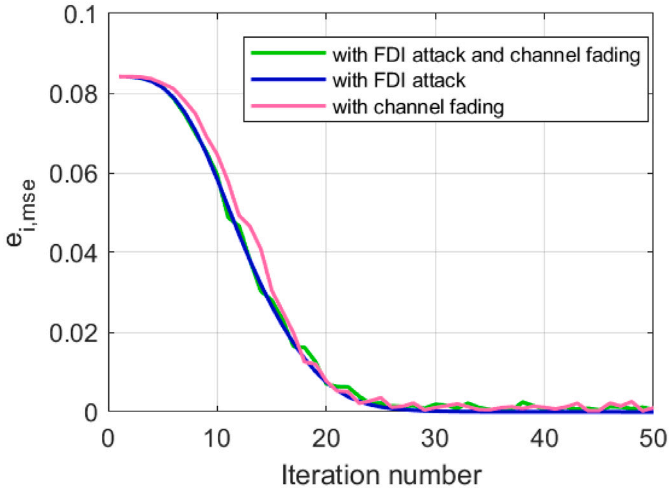

Fig. 2. MSE convergence curves of the system in different scenarios.

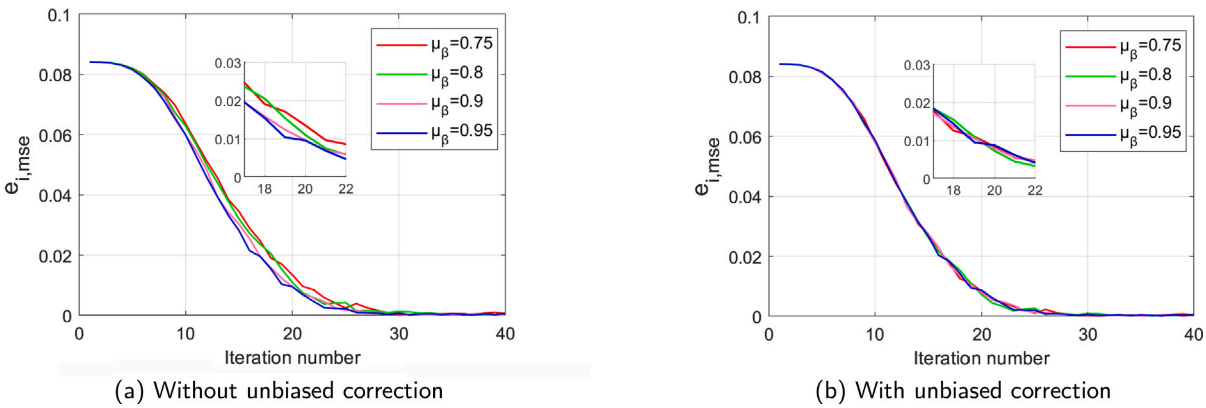

Fig. 3. System MSE convergence curves under different channel fading expectations with $\sigma_\beta = 0.05$.

fading coefficient μ_β and the standard deviation σ_β. A smaller μ_β indicates more severe average signal attenuation, while a larger σ_β means more intense random fluctuations of the faded signal. Fig. 3 depicts the system MSE convergence curves under different channel fading expectations without signal correction (a) and with signal correction (b), respectively. It can be observed from Fig. 3 that in the absence of correction, the smaller the expected value of channel fading (i.e., the more severe the channel fading), the slower the convergence speed, which is attributed to a significant reduction in effective gain. With the implementation of correction,

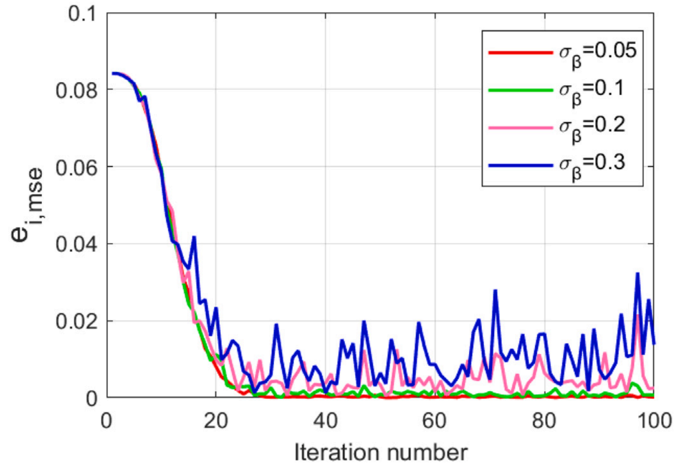

Fig. 4. System MSE convergence curves under different channel fading standard deviations with $\mu_\beta = 0.95$.

the error decay dynamics exhibit consistency across different fading expectations. A comparative analysis reveals that the correction mechanism counteracts the systematic effects induced by channel fading expectations, thus narrowing the discrepancies in the system's convergence speed under different expected values of the channel fading coefficient. Fig. 4 plots the error curves under different channel fading variances. The system can converge in all scenarios with varying variances, and the larger the variance, the slower the convergence speed and the higher the steady-state error.

5.2. Applications of single-link robots

The conventional ramp-type FDI attacks are mostly designed for slowly varying operating conditions of smart grids. However, the dynamic standard deviation embedded in the proposed attack model facilitates adaptive adjustment of the ramp increment rate, which renders the attack well applicable to the high-dynamic characteristics of robotic manipulators. Thus, to further corroborate the efficacy of the proposed control method in a practical nonlinear setting, a single-link robot simulation platform is established. Numerical experiments are performed to examine trajectory tracking accuracy and dynamic response. The following subsections describe the system configuration, experimental setup, and analysis of results. The dynamic equation of the system is described as

$$\ddot{\theta} = \frac{u - f\dot{\theta} - (m/2 + M)gL\sin(\theta)}{(ML^2 + I)/5.5}, \tag{35}$$

where $I = 1/3mL^2$, θ, $\dot{\theta}$, and $\ddot{\theta}$ respectively represent the rotational angular displacement, angular velocity, and angular acceleration of the single-link robot. u, f, m, M, g and L denote the motor torque, damping coefficient, load mass, link mass, gravitational acceleration, and link length, respectively.

To adapt to digital control scenarios, the continuous dynamic model is discretized by defining the state variables as $x = \theta$ and $y = \dot{\theta}$, and by applying the Euler discretization method. The resulting discrete-time model is given by

$$\begin{cases} x(t+1) = x(t) + hy(t), \\ y(t+1) = y(t) + \frac{h(u - fy(t) - (m/2+M)gL\sin(x(t)))}{(ML^2+I)/5.5}, \end{cases} \tag{36}$$

where h $= 0.01$s is the sampling time interval, and the system parameters are $f = 3$ kg·m^2/s, $m = 0.1$ kg, $M = 4$ kg, $g = 9.8$ m/s^2 and $L = 0.5$ m.

The desired trajectory y_d of the system is

$$y_d = 0.5\sin(2\pi t)(1 - exp(-5t)), \quad t \in [0, 2]. \tag{37}$$

Before the simulation experiment, we set $y_i(0) = 0$ as the initial output for each iteration $u_0(t) = 0$ as the control input for the first iteration at any time and $\varphi_i(\tau) = 0.4$ as the initial estimate of the parameter. In addition, we also set the controller parameters as $\rho = 1$, $\lambda = 0.5$, $\eta = 1.3$, and $\mu = 0.1$ respectively. The five designated moments are $t_1 = 0.4$, $t_2 = 0.8$, $t_3 = 1.2$, $t_4 = 1.6$ and $t_5 = 2$ respectively. Fig. 5 shows the convergence curves of the angular velocity MSE throughout the iterative process for the three control methods. Specifically, the parameters of the PPTPILC algorithm are configured consistently with those in Example 1. For the HOPTPILC algorithm, the key parameters are set as $r = 3$, $\alpha = [0.92, 0.072, 0.008]$ and $[\rho_4, \rho_5, \rho_6, \rho_7] = [0.8, 0.8, 0.6, 0.6]$. The results demonstrate that the proposed control strategy exhibits a notably faster convergence rate compared to the comparative methods.

To further verify the robustness of the proposed method against general transmission disturbances, zero-mean Gaussian white noise is added to the channel output. Fig. 6 presents the MSE convergence curves of the angular velocity tracking for the three methods under Gaussian white noise with different intensities ($\sigma = 0.03, 0.06, 0.09$). As the noise intensity increases, the tracking performance of all three methods degrades, with increased steady-state errors. However, the proposed PTPFILC consistently outperforms PPTPILC

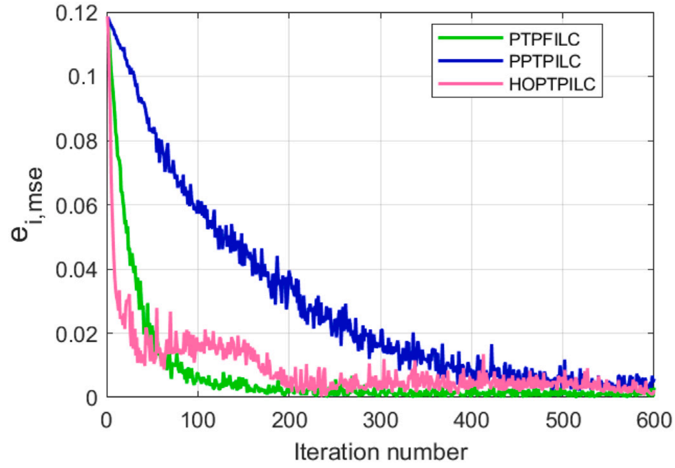

Fig. 5. Angular velocity MSE convergence curves of the single-link robot system.

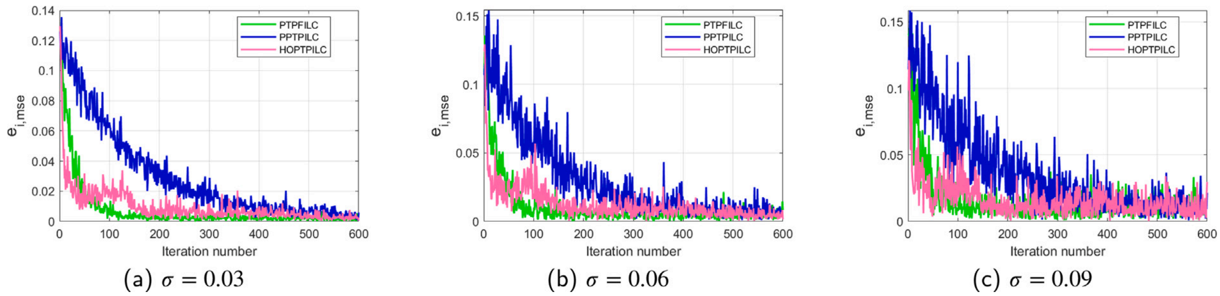

Fig. 6. Angular velocity MSE convergence curves of a single-link robot system under Gaussian white noise.

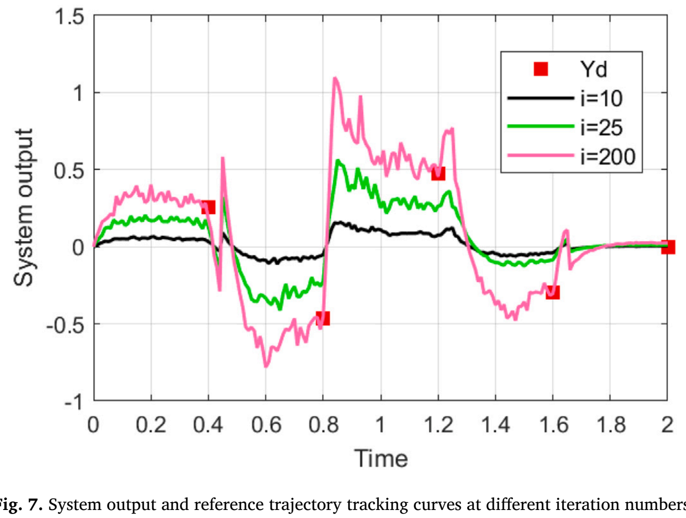

Fig. 7. System output and reference trajectory tracking curves at different iteration numbers.

and HOPTPILC in terms of convergence speed. Fig. 7 shows the tracking curves of the system output and reference trajectory at different iteration times. The results indicate that the more iterations, the closer the system output is to the reference trajectory, indicating that the iterative mechanism of the proposed method can continuously optimize the control effect and ultimately achieve high-precision tracking. Fig. 8 shows the convergence curve of MSE with iteration times when the attack coefficient takes different values. The results indicate that as α increases, the initial convergence rate slightly slows down, but the overall convergence trend is consistent. It also demonstrates that the proposed method has good robustness to the parameter α, and can achieve fast and stable error convergence within the value range of $\alpha = [3, 12]$.

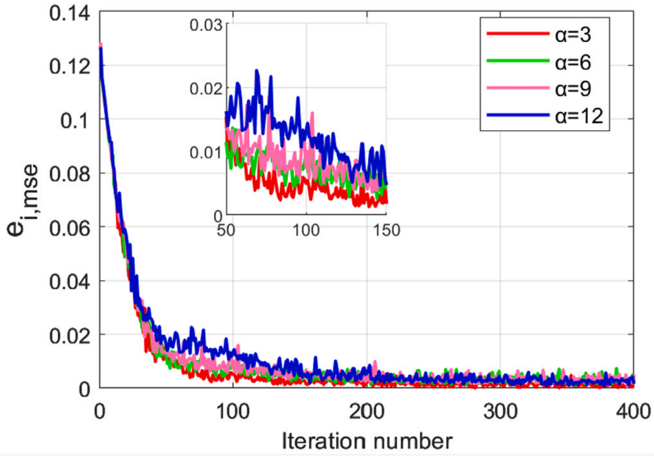

Fig. 8. MSE convergence curves of a single-link robot system under different FDI attack coefficients.

6. Conclusion

This paper has addressed the challenging data-driven tracking control problem for unknown nonlinear discrete-time repetitive systems operating under the severe dual threats of physical-layer FDI attacks and multiplicative communication channel fading. The core contribution lies in the synthesis of a novel, resilient data-driven PTPFILC framework. By organically integrating an unbiased signal correction mechanism to restore fading-distorted data with a dynamic dual-update strategy, the proposed scheme concurrently optimizes the control input and parameter estimation without relying on precise system dynamics. Rigorous theoretical analysis and comprehensive comparative simulations demonstrate that the proposed method consistently achieves high-precision PTP tracking within a finite iteration threshold. Furthermore, it exhibits exceptional robustness and stable error convergence against complex, coupled cyber-physical disturbances. Ultimately, these findings provide a highly practical and secure data-driven solution for PTP tracking of unknown nonlinear repetitive systems. However, it should be acknowledged that a limitation of the current framework is its reliance on the correct prior knowledge of the system's input–output control direction for the parameter reset mechanism. Building upon these insights, our future research will focus on developing adaptive direction estimation algorithms to solve the limitation, and extend this robust data-driven control paradigm to complex, large-scale multi-agent systems, with a particular focus on distributed resilient tracking under aperiodic cyber-attacks and severe communication constraints.

CRediT authorship contribution statement

Lijuan Zha: Writing – review & editing. **Shuyi Huang:** Writing – original draft. **Jinliang Liu:** Writing – review & editing. **Chen Peng:** Writing – review & editing.

Declaration of competing interest

The authors declare that they have no known competing financial interests or personal relationships that could have appeared to influence the work reported in this paper.

Data availability

No data were used for the research described in the article.

References

[1] S. Sui, C. Chen, S. Tong, Command filter-based predefined time adaptive control for nonlinear systems, IEEE Trans. Autom. Control 69 (2024) 7863–7870.
[2] N. Zhang, J. Chen, F. Viadero-Monasterio, H. Zhang, Iterative learning distributed model predictive control for autonomous vehicle platoons with applications to repetitive tasks, IEEE Trans. Intell. Transp. Syst. 26 (2025) 20882–20896.
[3] N. Lin, R. Chi, B. Huang, Double-layered iterative learning control for nonlinear systems, IEEE Trans. Syst. Man Cybern. Syst 54 (2024) 6033–6042.
[4] K. Nie, R. Langari, Performance-based iterative velocity updating method for robot-assisted upper limb training in reaching motions, IEEE Robot. Autom. Lett. 11 (2026) 2058–2065.
[5] T. Liu, D. Shen, J. Wang, Adaptive quantized iterative learning control using encoding-decoding strategy, IEEE Trans. Cybern. 55 (2025) 1359–1371.
[6] C. Lu, D. Meng, H. Li, Data-induced learning control for unknown nonlinear systems with full-tracking performances, Sci. China Inf. Sci. 68 (2025) 182201.
[7] H. Tao, J. Li, Y. Chen, V. Stojanovic, H. Yang, Robust point-to-point iterative learning control with trial-varying initial conditions, IET Control Theory Appl. 14 (2020) 3344–3350.
[8] M. Kakavand, M.H. Bibalan, On the effective capacity of fractional order Rayleigh fading channels: an analytical approach, Digit. Signal Process. 180 (2026) 106221.
[9] H. Chen, Y. Xiao, S. Fang, G. Wu, Low-complexity transmit antenna selection for offset spatial modulation, Sci. China Inf. Sci. 65 (2022) 192302.
[10] X. Li, G. Wei, L. Wang, Distributed set-membership filtering for discrete-time systems subject to denial-of-service attacks and fading measurements: a zonotopic approach, Inf. Sci. 547 (2021) 49–67.

[11] L. Su, V. Gupta, G. Chesi, Stabilization of linear systems across a time-varying AWGN fading channel, IEEE Trans. Autom. Control 65 (2020) 4902–4907.
[12] J. Liu, Z. Liu, Y. Li, E. Tian, C. Peng, Privacy-protected formation control for unmanned surface vehicles: a neural predictor-based noncooperative game framework, IEEE Trans. Veh. Technol. (2026), https://doi.org/10.1109/TVT.2026.3651837
[13] L. Yin, L. Xu, F. Hou, H. Zhu, H. Jing, X. Sun, C. Wu, Security analysis and control under periodic DoS attacks, IEEE Internet Things J. 11 (2024) 8473–8484.
[14] J. Liu, E. Ma, L. Zha, E. Tian, Distributed energy management for microgrids: when privacy preservation meets multiple mechanisms, IEEE Trans. Consum. Electron. 72 (2026) 1514–1523.
[15] J. Li, X. Li, Z. Cheng, H. Ren, H. Li, Event-based secure control for cyber-physical systems against false data injection attacks, Inf. Sci. 679 (2024) 121093.
[16] C. Xu, H. Dong, Y. Shen, J. Li, Dynamic event-triggered fault estimation for complex networks with time-correlated fading channels, Inf. Sci. 644 (2023) 119288.
[17] K. Yang, D. Liu, S. Baldi, W. Yu, C. Lv, Decoupling-based resilient control of vehicular platoons under injection of false wireless data, IEEE Trans. Intell. Transp. Syst. 25 (2024) 21500–21514.
[18] J. Liu, S. Mao, L. Zha, E. Tian, C. Peng, Privacy-preserving and collision-free formation control for heterogeneous multiagent systems, IEEE Trans. Consum. Electron. (2026), https://doi.org/10.1109/TCE.2026.3667772
[19] H. Ali, R. Safdar, W. Ding, Y. Zhou, Y. Yao, L. Yao, F. Gao, Intelligent machine learning-based multi-model fusion monitoring: application to industrial physio-chemical systems, Control Eng. Pract. 162 (2025) 106361.
[20] H. Ali, F. Gao, Fault detection and diagnosis using reconstruction-based DiGLPP: application to industrial distillation system, IFAC-PapersOnLine. 59 (2025) 187–192.
[21] H. Ali, R. Safdar, Y. Zhou, Y. Yao, L. Yao, Z. Zhang, W. Ding, F. Gao, A novel dynamic machine learning-based explainable fusion monitoring: application to industrial and chemical processes, Mach. Learn.: Sci. Technol. 6 (2024) 015005.
[22] X. Bu, C. Yang, L. Lv, J. Liang, Z. Hou, Data-driven point-to-point finite-iteration learning control for a class of nonlinear systems with output saturation, IEEE Trans. Cybern. 55 (2025) 5492–5503.
[23] X. Zhang, Z. Hou, Data-driven predictive point-to-point iterative learning control, Neurocomputing 518 (2023) 431–439.
[24] N. Lin, H. Peng, R. Chi, Event-triggered data-driven iterative learning control for multiagent systems with FDI attacks, IEEE Internet Things J. 12 (2025) 22036–22047.
[25] C. Fei, J. Shen, H. Qiu, Z. Zhang, Data driven secure control for cyber-physical systems under hybrid attacks: a Stackelberg game approach, J. Franklin Inst. 361 (2024) 106715.
[26] Y. Yin, W. Yu, X. Bu, Q. Yu, Security data-driven iterative learning control for unknown nonlinear systems with hybrid attacks and fading measurements, ISA Trans. 129 (2022) 1–12.
[27] C. Liu, X. Ruan, Y. Liu, C. Chien, Optimization-based iterative learning control scheme for point-to-point tracking of nonlinear systems, Nonlinear Dyn. 113 (2025) 2487–2503.
[28] K. Nagaraj, N. Aljohani, S. Zou, T. Zou, A. Bretas, J. McNair, A. Zare, Smart FDI attack design and detection with data transmutation framework for smart grids, in: In 2021 IEEE Power Energy Society General Meeting (PESGM), 2021, pp. 1–5.
[29] Y. Zhang, B. Lei, M. Rajabinezhad, C. Ding, S. Zuo, Observer-based data-driven consensus control for nonlinear multi-agent systems against denial-of-service and false data injection attacks, J. Dyn. Syst. Meas. Control. 148 (2025) 031007.
[30] S. Huang, D. Shen, J. Wang, Point-to-point learning tracking control via fading communication using reference update strategy, IEEE Trans. Cybern. 54 (2024) 2284–2294.
[31] X. Zhang, M. Hou, Z. Hou, Data-driven high-order point-to-point ILC with higher computational efficiency, IEEE Trans. Autom. Sci. Eng. 21 (2024) 6011–6026.